Results in Applied Mathematics 8 (2020) 100098

Contents lists available at ScienceDirect

Results in Applied Mathematics

journal homepage: www.elsevier.com/locate/results-in-applied-mathematics

Analysis of methods for the Maxwell-random Lorentz model

Andrew Fisher [a,1], Jacqueline Alvarez [b,1], N.L. Gibson [c,*,1]

[a] University of California, Los Angeles, United States of America
[b] University of California, Merced, United States of America
[c] Oregon State University, United States of America

ARTICLE INFO

Article history:
Received 31 December 2019
Received in revised form 8 February 2020
Accepted 12 February 2020
Available online 3 March 2020

Keywords:
Lorentz polarization
Polynomial Chaos
FDTD
Maxwell's equations

ABSTRACT

Maxwell's equations describes the propagation of electromagnetic fields in materials. Constitutive laws are used to describe the material response to the fields. We extend a novel computational framework involving Polynomial Chaos Expansions to the Lorentz model including random parameters. We perform stability and dispersion analyses for the resulting fully discrete schemes utilizing the second order Yee scheme in two spatial dimensions.

1. Introduction

Electromagnetic interrogation of dispersive materials is of current interest in industry for its potential as a non-invasive method in identifying weaknesses or compositions in materials. An example is determining a material's dispersive properties through the analysis of a single transmitted ultra-wideband (UWB) pulse. Several different methods have been suggested that expand on the common Lorentz polarization model, some employing linear combinations of poles or normally distributed poles to fit data [1]. In this paper, however, we explore placing beta distributions on the dielectric parameters in the model. A recently rediscovered modeling framework allows uncertainty at the molecular level to enter via distributions of parameters representing variability [2]. Numerous experimental efforts have been pursued to describe electromagnetic measurements for materials in the frequency domain with distributions of dielectric parameters, especially relaxation times in multiple Debye models. A significant amount of this work is reviewed in the survey paper by Foster and Schwan [3].

First we present necessary background information including Maxwell's equations, the constitutive equations, and the Lorentz model. Next we define random polarization including distributions of dielectric parameters. For analysis in the time domain, we use Polynomial Chaos [4–6] and the Finite Difference Time Domain (FDTD) [7,8] method to discretize for a dispersive medium [9–12]. Finally we show the stability of the random Lorentz model and its discretization, and perform a dispersion analysis in a manner similar to [2] for the Random Debye model.

* Corresponding author.
E-mail addresses: andrew.fisher@physics.ucla.edu (A. Fisher), jalvarez94@ucmerced.edu (J. Alvarez), gibsonn@math.oregonstate.edu (N.L. Gibson).

[1] Funding: This work was performed during the 2017 REU program in mathematics at Oregon State University, with support by National Science Foundation Grant DMS-1359173.

https://doi.org/10.1016/j.rinam.2020.100098

2. Background

2.1. Maxwell's equations

We begin by presenting Maxwell's equations that describe the behavior of electromagnetic waves in free space. D and B are the electric and magnetic flux densities, E and H are the electric and magnetic fields, J is the conduction current density, and ρ is the charge density

$$\frac{\partial D}{\partial t} + J = \nabla \times H \tag{1a}$$

$$\frac{\partial B}{\partial t} = -\nabla \times E \tag{1b}$$

$$\nabla \cdot D = \rho \tag{1c}$$

$$\nabla \cdot B = 0. \tag{1d}$$

Next, we incorporate the constitutive laws that adapt Maxwell's equations for propagation in materials. Additionally, $\tilde{\epsilon}$ is electric permittivity and is equal to the product of the permittivity of free space and relative permittivity ($\tilde{\epsilon} = \epsilon_0 \epsilon$). Magnetic permeability is given by μ, the material's polarization and conductivity are P and σ, and J_s is the source current

$$D = \tilde{\epsilon} E + P \tag{2a}$$

$$B = \mu H + M \tag{2b}$$

$$J = \sigma E + J_s. \tag{2c}$$

To find the equations defining electromagnetic waves in a material, we substitute the constitutive equations into Maxwell's curl equations:

$$\tilde{\epsilon} \frac{\partial E}{\partial t} = \nabla \times H - J - \frac{\partial P}{\partial t} = \nabla \times H - \sigma E - J_s - \frac{\partial P}{\partial t} \tag{3}$$

$$\mu \frac{\partial H}{\partial t} = -\nabla \times E - \frac{\partial M}{\partial t}. \tag{4}$$

For convenience of notation, we restrict our discussion in this section to the one dimensional case with waves propagating in the z-direction, however, the Yee Scheme and Polynomial Chaos Expansions apply in a similar manner to 2D and 3D. Because electromagnetic waves are transverse with the electric and magnetic fields oscillating perpendicular to each other, we choose E and H to oscillate in the x and y directions, respectively. Prior to interrogation, there are no fields or polarizations present so our initial conditions are:

$$E(0, z) = H(0, z) = P(0, z) = 0. \tag{5}$$

Our boundary conditions include the interrogating signal, $f_b(t)$, at $z = 0$ and a reflective surface at $z = z_0$:

$$E(t, 0) = f_b(t) \text{ and } E(t, z_0) = 0. \tag{6}$$

We also assume that our material is non-conducting with no magnetization or source current ($\sigma = 0$, $M = 0$, $\mu = \mu_0$ and $J_s = 0$):

$$\tilde{\epsilon} \frac{\partial E_x}{\partial t} = -\frac{\partial H_y}{\partial z} - \frac{\partial P_x}{\partial t} \tag{7a}$$

$$\mu_0 \frac{\partial H_y}{\partial t} = -\frac{\partial E_x}{\partial z}. \tag{7b}$$

where μ_0 is the magnetic permeability of free space. From now on, we drop the subscripts so that $E = E_x$, $P = P_x$, and $H = H_y$.

2.2. Lorentz model

There are several models that describe polarization in materials. In this paper, we focus on the Lorentz model for which the physical assumption is that we can treat electrons in the material as simple harmonic oscillators (i.e. electrons attached to little springs) [13]. We can then write down the second order differential equation for a damped, driven oscillator where ν is the damping coefficient, ω_0 is the natural resonant frequency, and x is the displacement:

$$m\ddot{x} + 2m\nu\dot{x} + m\omega_0^2 x = F_{driving}. \tag{8}$$

Recall that polarization can be defined as the electric dipole moment density and that the dipole moment between two equal charges is the product of their charge and displacement ($\vec{p} = q\vec{x}$). Then letting N be the electron density and $F_{driving} = q\vec{E}$, we convert (8) into a differential equation relating the polarization and electric field:

$$\ddot{P} + 2\nu\dot{P} + \omega_0^2 P = \epsilon_0 \omega_p^2 E \quad \text{with} \quad \omega_p^2 = Nq^2/m\epsilon_0. \tag{9}$$

It is helpful to note that ν and ω_p can be expressed in terms of a time constant τ and static permittivity ϵ_s where $\nu = \frac{1}{2\tau}$ and $\omega_p^2 = \omega_0^2(\epsilon_s - \epsilon_\infty)$ [13]. Using either Fourier or Laplace transforms, we may express the polarization in terms of a convolution of the electric field:

$$P = \int_0^t g(t-s,x)E(s,x)dx \tag{10a}$$

$$g = \frac{\epsilon_0\omega_p^2}{\nu_0}e^{-\nu t}\sin\nu_0 t \quad \text{and} \quad \nu_0 = \sqrt{\omega_0^2 - \nu^2}. \tag{10b}$$

The function g is the dielectric response function (DRF) and is responsible for how the polarization reacts to past electric fields. In other words, it encompasses the polarization's memory of the electric field. Plugging equation (9) into (2a) and taking the Fourier transform, we get $\hat{D} = \epsilon_0\epsilon(\omega)\hat{E}$ where $\epsilon(\omega)$ is the complex permittivity given by

$$\epsilon(\omega) = \epsilon_\infty + \frac{\omega_p^2}{\omega_0^2 - \omega^2 + i2\nu\omega}. \tag{11}$$

For multiple poles, the permittivity merely includes a summation:

$$\epsilon(\omega) = \epsilon_\infty + \sum_{i=1}^{\infty}\frac{\omega_{p,i}^2}{\omega_{0,i}^2 - \omega^2 + i2\nu_i\omega}. \tag{12}$$

2.3. Random polarization

In this paper, we research the effects of altering the original Lorentz model by applying a probability distribution to one of the parameters. As mentioned earlier, one (or more) of the material parameters in the Lorentz model could be assumed to have microscale variation which could be modeled with probability distributions. If one of the material parameters is random, then so will be the polarization and the complex permittivity. We define the random Lorentz model similar to (9) and (11), but where the material parameter is now a random variable and $\mathcal{P}$ is the random polarization:

$$\ddot{\mathcal{P}} + 2\nu\dot{\mathcal{P}} + \omega_0^2\mathcal{P} = \epsilon_0\omega_p^2 E \tag{13}$$

and

$$\epsilon(\omega) = \epsilon_\infty + \frac{\omega_p^2}{\omega_0^2 - \omega^2 + i2\nu\omega}. \tag{14}$$

Next, we define the macroscopic polarization of (7a) as the expected value of the random polarization where the random parameter is given in terms of a random variable ξ defined over [a,b] with probability density function $f(\xi)$ [14]:

$$P(t,z) = \int_a^b \mathcal{P}(t,z;\xi)f(\xi)d\xi. \tag{15}$$

We emphasize that Maxwell's equations (7) depend only on the expected value of the random polarization, and therefore remain deterministic in this model. If we were to allow ϵ or μ to be random, or random initial or boundary conditions, then a stochastic Maxwell's equation [15–17] would result.

In [18] it was determined that a parameter that should be considered variable in a material is ω_0, therefore we make this assumption in the current work. In Fig. 1 we show a simulation of the electric field which is coupled to the expected value of the random Lorentz polarization, compared to the electric field which is coupled to a deterministic Lorentz model for the polarization using only the average parameter value. The distribution on ω_0 makes an appreciable difference in both amplitude and phase. Since the parameter ω_0 always appears as ω_0^2, we choose to vary ω_0^2 for simplicity. See [19] for estimation of the distribution of parameters using complex permittivity as well as time-domain data.

3. Polynomial Chaos

3.1. Polynomial expansion

Now we consider the time domain formulation of the random Lorentz model, using Polynomial Chaos to deal with the random variable ω_0^2. Polynomial Chaos is a method for approximating solutions to random differential equations by expressing quantities as orthogonal polynomial expansions in the random variable [6]. We expand in the normalized Jacobi polynomials (of which, Legendre polynomials are a special case), but because they are defined on $[-1,1]$ it is necessary to scale our distribution. Letting $\omega_0^2 = m + r\xi$ so that ξ is defined on $[-1,1]$, we identify m and r as the center and radius of the distribution. The random polarization can now be expressed as a function of ξ,

$$\mathcal{P}(\xi,t) = \sum_{i=0}^{\infty}\alpha_i(t)\phi_i(\xi). \tag{16}$$

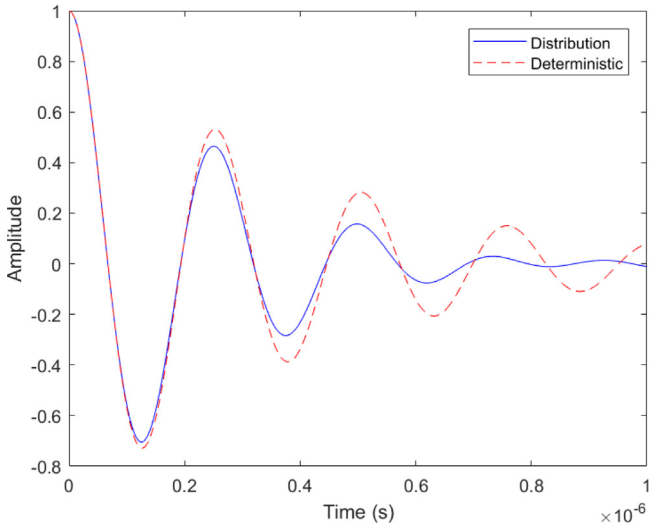

Fig. 1. Simulation of expected value of random Lorentz model compared to the Lorentz model with average parameters.

All orthogonal polynomials also satisfy a recurrence relationship,

$$\xi\phi_n(\xi) = a_n\phi_{n+1}(\xi) + b_n\phi_n(\xi) + c_n\phi_{n-1}(\xi) \tag{17}$$

where the coefficients for the Jacobi polynomials are:

$$a_n = \frac{2(n+\hat{\alpha})(n+\hat{\beta})}{(2n+\hat{\alpha}+\hat{\beta})(2n+\hat{\alpha}+\hat{\beta}+1)}$$
$$b_n = \frac{\hat{\beta}^2-\hat{\alpha}^2}{(2n+\hat{\alpha}+\hat{\beta})(2n+\hat{\alpha}+\hat{\beta}+2)}$$
$$c_n = \frac{2(n+1)(n+\hat{\alpha}+\hat{\beta}+1)}{(2n+\hat{\alpha}+\hat{\beta}+1)(2n+\hat{\alpha}+\hat{\beta}+2)},$$

where $\hat{\alpha}$ and $\hat{\beta}$ are parameters of the orthogonal polynomial family and are analogous to shape parameters in the Beta probability distribution.

Plugging (16) into (13) and replacing ω_0^2 with $m + r\xi$ gives,

$$\sum_{i=0}^{\infty} \ddot{\alpha}_i(t)\phi_i(\xi) + 2\nu\dot{\alpha}_i(t)\phi_i(\xi) + (r\xi + m)\alpha_i(t)\phi_i(\xi) = \epsilon_0\omega_p^2 E\phi_0(\xi). \tag{18}$$

Then separating and using the recurrence relation (17), we have

$$\sum_{i=0}^{\infty} \left[\ddot{\alpha}_i(t) + 2\nu\dot{\alpha}_i(t) + m\alpha_i(t)\right]\phi_i(\xi)$$
$$+r\sum_{i=0}^{\infty} \alpha_i(t)\left[a_i\phi_{i+1}(\xi) + b_i\phi_i(\xi) + c_i\phi_{i-1}(\xi)\right] = \epsilon_0\omega_p^2 E\phi_0(\xi). \tag{19}$$

Taking the weighted inner product with $\phi_j(\xi)$ for $j = 0 \ldots p-1$, we have

$$\sum_{i=0}^{p-1} \left[\ddot{\alpha}_i(t) + 2\nu\dot{\alpha}_i(t) + m\alpha_i(t)\right]\langle\phi_i, \phi_j\rangle$$
$$+r\sum_{i=0}^{p-1} \alpha_i(t)\left[a_i\langle\phi_{i+1}, \phi_j\rangle + b_i\langle\phi_i, \phi_j\rangle + c_i\langle\phi_{i-1}, \phi_j\rangle\right] = \langle\epsilon_0\omega_p^2 E\phi_0, \phi_j\rangle \tag{20}$$

where $\langle \phi_i, \phi_j \rangle$ for the normalized Jacobi polynomials is defined as:

$$\langle \phi_i, \phi_j \rangle := \int_{-1}^{1} \phi_i(\xi)\phi_j(\xi)w(\xi)d\xi = \begin{cases} 0 & \text{if } i \neq j \\ 1 & \text{if } i = j. \end{cases} \tag{21}$$

Because we have projected onto a finite number of basis polynomials, we can now express our system in matrix notation:

$$\ddot{\vec{\alpha}} + 2\nu\dot{\vec{\alpha}} + A\vec{\alpha} = \vec{f} \tag{22}$$

where $A = rM + mI$,

$$M = \begin{pmatrix} b_0 & c_1 & 0 & \cdots & 0 \\ a_0 & b_1 & c_2 & & \vdots \\ 0 & \ddots & \ddots & \ddots & 0 \\ \vdots & & a_{p-3} & b_{b-2} & c_{p-1} \\ 0 & \cdots & 0 & a_{p-2} & b_{p-1} \end{pmatrix} \text{ and } \vec{f} = \hat{e}_1\epsilon_0\omega_p^2 E$$

and $\hat{e}_1$ is the first standard column unit vector.

Letting $\dot{\vec{\alpha}} = \vec{\beta}$ we may express (22) as a system of differential equations:

$$\dot{\vec{\alpha}} = \vec{\beta} \tag{23a}$$

$$\dot{\vec{\beta}} = -A\vec{\alpha} - 2\nu\vec{\beta} + \vec{f}. \tag{23b}$$

Note that the deterministic value $\vec{f}$ forces the system and is dependent on the electric field governed by Maxwell's equations. Maxwell's equations are coupled to the macroscopic polarization, i.e., the expected value of the random polarization at each point (t, z), which is well approximated by

$$P(t, z; F) = \mathbb{E}[\mathcal{P}] \approx \alpha_o(t, z), \tag{24}$$

where the F notation indicates that there is a dependence on the choice of probability distribution.

4. Forward simulation time domain

4.1. FDTD discretization

Combining Maxwell's equations with our results from Polynomial Chaos, we have the four equations that completely determine propagation through a dielectric material. We repeat them here as a reference:

$$\epsilon_\infty\epsilon_0\frac{\partial E}{\partial t} = -\frac{\partial H}{\partial z} - \beta_0 \tag{25a}$$

$$\frac{\partial H}{\partial t} = -\frac{1}{\mu_0}\frac{\partial E}{\partial z} \tag{25b}$$

$$\dot{\vec{\alpha}} = \vec{\beta} \tag{25c}$$

$$\dot{\vec{\beta}} = -A\vec{\alpha} - 2\nu\vec{\beta} + \vec{f}. \tag{25d}$$

It is important to note that $\frac{\partial P}{\partial t}$ is the time rate of change in the macroscopic polarization, or the time rate of change of the expected value of the random polarization. Since the 0th Jacobi polynomial approximates the expected value of the expansion, we identify $\beta_0 = \frac{\partial P}{\partial t}$. This explains our substitution in (25a).

To model these equations, we discretize them according to the one-dimensional Yee Scheme [7]. The Yee Scheme implements a staggered grid where the electric field and random polarization are evaluated at integer time steps and spatial steps, while the magnetic field is evaluated at half integer time steps and spatial steps. We consider the domain $z \in [0, z_0]$ for $t \in [0, T]$, choosing integers j_{max} and n_{max} to discretize so that $\Delta z = z_0/j_{max}$ and $\Delta t = T/n_{max}$. Let $z_j = j\Delta z$ and $t^n = n\Delta t$. If U is a field variable, we define the *grid functions*, or the numerical approximations, as

$$U_j^n \approx U(z_j, t^n).$$

Our discrete initial conditions and boundary conditions are:

$$E_j^0 = \vec{\alpha}_j^0 = \vec{\beta}_j^0 = 0 \text{ for } 0 \leq j \leq j_{max}, \quad H_j^n = 0 \text{ for } 0 \leq j \leq j_{max} \text{ and } n \leq 0,$$

$$E_0^n = f_b(t^n) \text{ and } E_{j_{max}}^n = 0 \text{ for } 0 \leq n \leq n_{max}$$

for some given boundary value function $f_b(t)$.

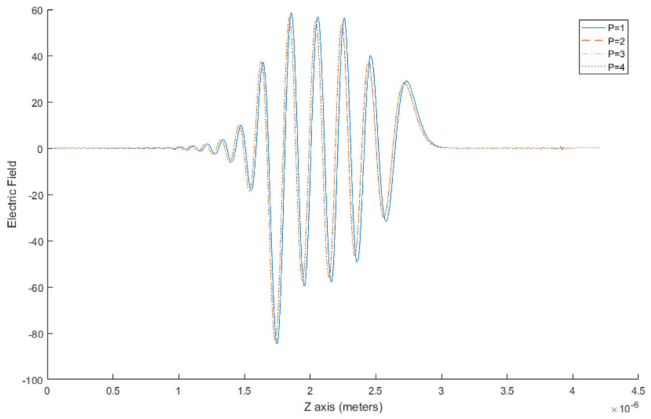

(a)

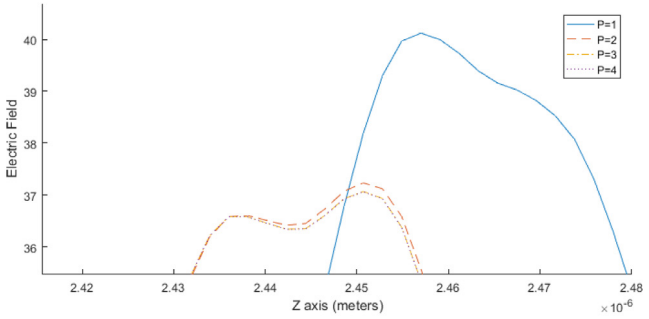

(b)

Fig. 2. P-convergence of forward simulation at $t = 1.4 \times 10^{-5}$ ns, (b) is a zoom of (a).

First we approximate derivatives with finite differences and constant terms with averages:

$$\epsilon_\infty \epsilon_0 \frac{E_j^{n+1} - E_j^n}{\Delta t} = -\frac{H_{j+\frac{1}{2}}^{n+\frac{1}{2}} - H_{j-\frac{1}{2}}^{n+\frac{1}{2}}}{\Delta z} - \frac{\beta_{0,j}^{n+1} + \beta_{0,j}^n}{2} \tag{26a}$$

$$\frac{H_{j+\frac{1}{2}}^{n+\frac{1}{2}} - H_{j+\frac{1}{2}}^{n-\frac{1}{2}}}{\Delta t} = -\frac{1}{\mu_0} \frac{E_{j+1}^n - E_j^n}{\Delta z} \tag{26b}$$

$$\frac{\vec{\alpha}_j^{n+1} - \vec{\alpha}_j^n}{\Delta t} = \frac{\vec{\beta}_j^{n+1} + \vec{\beta}_j^n}{2} \tag{26c}$$

$$\frac{\vec{\beta}_j^{n+1} - \vec{\beta}_j^n}{\Delta t} = -A \frac{\vec{\alpha}_j^{n+1} + \vec{\alpha}_j^n}{2} - 2\nu \frac{\vec{\beta}_j^{n+1} + \vec{\beta}_j^n}{2} + \frac{\hat{e}_1 \epsilon_0 \omega_p^2}{2} \left[E_j^{n+1} + E_j^n \right]. \tag{26d}$$

Eqs. (26a), (26c), and (26d) are defined for $\{1 \le j \le j_{max} - 1,\ 0 \le n \le n_{max} - 1\}$ and (26b) is defined for $\{0 \le j \le j_{max} - 1,\ 0 \le n \le n_{max} - 1\}$.

4.2. Simulation convergence

We now show that the Polynomial Chaos method converges quickly in p. We assume the material parameters $\tau = 7 \times 10^{-16}$, $\omega_0 = 1.8 \times 10^{16}$, and $\omega_p = 2 \times 10^{16}$ from [13]. We choose the time step to sufficiently resolve the smallest time scale, which in this problem is $T_p := 2\pi/\omega_p$. Specifically, we used $\Delta t = 0.0005 T_p$, or 1.7×10^{-19} (note that computations were actually performed in scaled time). The spatial step was chosen to satisfy the CFL constraint, specifically $\Delta z = \frac{1}{2} c\ \Delta t$, where c is the speed of light in a vacuum.

Choosing the interrogating signal as a sine wave with angular frequency of 6×10^{15} and duration of 5 periods, we plot the signals at $t = 1.4 \times 10^{-5}$ ns for four different p values in Fig. 2. Note that $p = 1$ corresponds to a deterministic model, ignoring the distribution entirely. The signals for $p = 3$ and $p = 4$ are indistinguishable on the plots. The approximate relative errors of $p = 2$ and $p = 3$ compared to $p = 4$ are .56% and 0.014%, respectively. Thus, an expansion of three

polynomials accurately approximates the convergence for large p. However, due to the high resonant frequencies of Lorentz materials, time steps and simulations must be very short. Therefore, small discrepancies might lead to more significant errors on a larger simulation.

5. Stability

5.1. 2D random Lorentz model

Here we show the stability of the random Lorentz model in a two dimensional domain $\mathcal{D}$, similar to the work for the random Debye model in [20]. However, the analysis could easily be generalized to three dimensions. First, we give Maxwell's Equations for two dimensions along with the random Lorentz differential equation written as a system of first order equations. To do this, we define the scalar curl operator on a vector field $\mathbf{U} = (U_x, U_y)^T$ as curl $\mathbf{U} = \frac{\partial U_y}{\partial x} - \frac{\partial U_x}{\partial y}$, and the vector curl operator on the scalar field V to be $\mathbf{curl}\ V = \left(\frac{\partial V}{\partial y}, -\frac{\partial V}{\partial x}\right)^T$.

$$\mu_0 \frac{\partial H}{\partial t} = -\ \text{curl}\ \mathbf{E} \tag{27a}$$

$$\epsilon_0 \epsilon_\infty \frac{\partial \mathbf{E}}{\partial t} = \mathbf{curl}\ H - \mathbf{J} \tag{27b}$$

$$\frac{\partial \mathcal{P}}{\partial t} = \mathcal{J} \tag{27c}$$

$$\frac{\partial \mathcal{J}}{\partial t} = -2\nu\mathcal{J} - \omega_0^2 \mathcal{P} + \epsilon_0 \omega_p^2 \mathbf{E}, \tag{27d}$$

where $\mathbf{J} := \mathbb{E}[\mathcal{J}]$.

Next we define the vector spaces,

$$H(\text{curl}, \mathcal{D}) = \{\mathbf{u} \in \left(L^2(\mathcal{D})\right)^2 ;\ \text{curl}\ \mathbf{u} \in L^2(\mathcal{D})\} \tag{28}$$

$$H_0(\text{curl}, \mathcal{D}) = \{\mathbf{u} \in H(\text{curl}, \mathcal{D}), \mathbf{n} \times \mathbf{u} = 0\} \tag{29}$$

where $(\cdot, \cdot)_2$ and $\|\cdot\|_2$ denote the L^2 inner product and norm. Note that the boundary restriction of H_0 for an electric field is equivalent to a perfect electric conducting (PEC) boundary condition. This PEC condition is necessary so that Green's formula for the **curl** operator holds

$$(\mathbf{curl}\ H, \mathbf{u}) = (H, \text{curl}\ \mathbf{u})\ ,\ \forall \mathbf{u} \in H_0(\text{curl}, \mathcal{D}). \tag{30}$$

We also introduce the Hilbert space $V_F = (L^2(\Omega))^2 \otimes (L^2(\mathcal{D}))^2$ where Ω is the support of the distribution, [a,b], on ω_0^2. The inner product and norm are defined as follows:

$$(u, v)_F = \mathbb{E}[(u, v)_2]$$
$$\|u\|_F^2 = \mathbb{E}[\|u\|_2^2].$$

We note that this inner product and norm thus involve integration over $\mathcal{D}$ and Ω.

Multiplying (27a) by $v \in L^2(\mathcal{D})$, (27b) by $\mathbf{u} \in H_0(\text{curl}, \mathcal{D})$, (27c) and (27d) by $\mathbf{w_1}, \mathbf{w_2} \in \left(L^2(\mathcal{D})\right)^2$, and integrating over the domain $\mathcal{D}$, we arrive at the weak formulation:

$$\left(\mu_0 \frac{\partial H}{\partial t}, v\right)_2 = (-\text{curl}\ \mathbf{E}, v)_2 \tag{31a}$$

$$\left(\epsilon_0 \epsilon_\infty \frac{\partial \mathbf{E}}{\partial t}, \mathbf{u}\right)_2 = (\mathbf{curl}\ H, \mathbf{u})_2 - (\mathbf{J}, \mathbf{u})_2 \tag{31b}$$

$$\left(\frac{\partial \mathcal{P}}{\partial t}, \mathbf{w_1}\right)_F = (\mathcal{J}, \mathbf{w_1})_F \tag{31c}$$

$$\left(\frac{\partial \mathcal{J}}{\partial t}, \mathbf{w_2}\right)_F = (-2\nu\mathcal{J}, \mathbf{w_2})_F + \left(-\omega_0^2 \mathcal{P}, \mathbf{w_2}\right)_F + \left(\epsilon_0 \omega_p^2 \mathbf{E}, \mathbf{w_2}\right)_F . \tag{31d}$$

We now have all the tools to prove stability for the 2D random Lorentz model.

Theorem 5.1. *Let $\mathcal{D} \subset \mathbb{R}^2$ and suppose that $\mathbf{E} \in C(0, T; H_0(\text{curl}, \mathcal{D})) \cap C^1(0, T; (L^2(\mathcal{D}))^2)$, $\mathcal{P}, \mathcal{J} \in C^1(0, T; (V_F)^2)$, and $H(t) \in C^1(0, T; L^2(\mathcal{D}))$ are solutions of the weak formulation (31) for the Maxwell–Lorentz system (27) along with PEC boundary conditions. Then the system exhibits energy decay*

$$\mathcal{E}(t) \leq \mathcal{E}(0)\ \ \forall t \geq 0, \tag{32}$$

where the energy $\mathcal{E}(t)$ is defined as

$$\mathcal{E}(t) = \left(\left\| \sqrt{\mu_0}\, H(t) \right\|_2^2 + \left\| \sqrt{\epsilon_0 \epsilon_\infty}\, \mathbf{E}(t) \right\|_2^2 + \left\| \frac{\omega_0}{\omega_p \sqrt{\epsilon_0}}\, \mathcal{P}(t) \right\|_F^2 + \left\| \frac{1}{\omega_p \sqrt{\epsilon_0}}\, \mathcal{J}(t) \right\|_F^2 \right)^{\frac{1}{2}}. \tag{33}$$

Proof. We choose $v = H$, $\mathbf{u} = \mathbf{E}$, $\mathbf{w_1} = \mathcal{P}$, and $\mathbf{w_2} = \mathcal{J}$ in (31), multiply (31c) by $\frac{\omega_0^2}{\epsilon_0 \omega_p^2}$, and multiply (31d) by $\frac{1}{\epsilon_0 \omega_p^2}$. Then add all four equations together, utilizing our definition of energy and Green's formula.

$$\begin{aligned} \frac{1}{2}\frac{d\mathcal{E}^2(t)}{dt} &= -\Big(\operatorname{curl} \mathbf{E}, H\Big)_2 + \Big(H, \operatorname{curl} \mathbf{E}\Big)_2 - \Big(\mathbf{J}, \mathbf{E}\Big)_2 + \left(\frac{\omega_0^2}{\epsilon_0 \omega_p^2}\mathcal{J}, \mathcal{P}\right)_F \\ &\quad + \left(\frac{-2\nu}{\epsilon_0 \omega_p^2}\mathcal{J}, \mathcal{J}\right)_F + \left(\frac{-\omega_0^2}{\epsilon_0 \omega_p^2}\mathcal{P}, \mathcal{J}\right)_F + (\mathbf{E}, \mathcal{J})_F \end{aligned} \tag{34}$$

$$= -\left\| \sqrt{\frac{2\nu}{\epsilon_0 \omega_p^2}}\, \mathcal{J} \right\|_F^2, \tag{35}$$

since $(\mathbf{E}, \mathcal{J})_F = (\mathbf{E}, \mathbb{E}[\mathcal{J}])_2 = (\mathbf{J}, \mathbf{E})_2$.

After cancellation, we are left with

$$\frac{d\mathcal{E}^2(t)}{dt} = -2\left\| \sqrt{\frac{2\nu}{\epsilon_0 \omega_p^2}}\, \mathcal{J} \right\|_F^2, \tag{36}$$

and rearranging, we get

$$\frac{d\mathcal{E}(t)}{dt} = \frac{-1}{\mathcal{E}(t)}\left\| \sqrt{\frac{2\nu}{\epsilon_0 \omega_p^2}}\, \mathcal{J} \right\|_F^2 \leq 0 \tag{37}$$

for $\mathcal{E}(t) \neq 0$. Therefore the energy, $\mathcal{E}(t)$, is non-increasing and $\mathcal{E}(t) \leq \mathcal{E}(0)\ \forall t > 0$. Further, the energy is conserved if $\nu = 0$, i.e., no damping. □

5.2. Maxwell-PC Lorentz-FDTD

5.2.1. Discretization

For our discrete approximation to converge to the true solution, it must be consistent and stable. Consistency is guaranteed by FDTD. To show the stability of the Lorentz-FDTD model in two dimensions, we borrow notation from [20] that will ease the proof. First, consider the space $(x, y) \in [0, a] \times [0, b]$ for $t \in [0, T]$. Choose integers ℓ_{max}, j_{max}, and n_{max} to discretize the space so that $\Delta x = a/\ell_{max}$, $\Delta y = b/j_{max}$, and $\Delta t = T/n_{max}$. Let $x_\ell = \ell \Delta x$, $y_j = j\Delta y$, and $t^n = n\Delta t$. We stagger three discrete meshes in the x and y directions, and two discrete meshes in the time domain:

$$\tau_h^{E_x} := \left\{ \left(x_{\ell+\frac{1}{2}}, y_j \right) | 0 \leq \ell \leq \ell_{max} - 1, 0 \leq j \leq j_{max} \right\} \tag{38}$$

$$\tau_h^{E_y} := \left\{ \left(x_\ell, y_{j+\frac{1}{2}} \right) | 0 \leq \ell \leq \ell_{max}, 0 \leq j \leq j_{max} - 1 \right\} \tag{39}$$

$$\tau_h^{H} := \left\{ \left(x_{\ell+\frac{1}{2}}, y_{j+\frac{1}{2}} \right) | 0 \leq \ell \leq \ell_{max} - 1, 0 \leq j \leq j_{max} - 1 \right\} \tag{40}$$

$$\tau_t^{E} := \left\{ \left(t^n \right) | 0 \leq n \leq n_{max} \right\} \tag{41}$$

$$\tau_t^{H} := \left\{ \left(t^{n+\frac{1}{2}} \right) | 0 \leq n \leq n_{max} - 1 \right\}. \tag{42}$$

The field variables are discretized on the following discrete meshes:

$$E_x, P_x \text{ on } \tau_h^{E_x}, \quad E_y, P_y \text{ on } \tau_h^{E_y}, \quad H \text{ on } \tau_h^{H}, \quad E_x, E_y, P_x, P_y \text{ on } \tau_t^{E}, \quad H \text{ on } \tau_t^{H}.$$

Let x_α, y_β be a node on any spatial mesh, and t^γ a node on either temporal mesh. If U is a field variable, we define the *grid functions*, or the numerical approximations, as

$$U_{\alpha,\beta}^{\gamma} \approx U(x_\alpha, y_\beta, t^\gamma).$$

We define the time difference operator and time averaging operator as

$$\delta_t U_{\alpha,\beta}^{\gamma} := \frac{U_{\alpha,\beta}^{\gamma+\frac{1}{2}} - U_{\alpha,\beta}^{\gamma-\frac{1}{2}}}{\Delta t} \tag{43}$$

$$\overline{U}_{\alpha,\beta}^{\gamma} := \frac{U_{\alpha,\beta}^{\gamma+\frac{1}{2}} + U_{\alpha,\beta}^{\gamma-\frac{1}{2}}}{2} \tag{44}$$

and the spatial difference operators in the x and y direction as

$$\delta_x U^{\gamma}_{\alpha,\beta} \coloneqq \frac{U^{\gamma}_{\alpha+\frac{1}{2},\beta} - U^{\gamma}_{\alpha-\frac{1}{2},\beta}}{\Delta x} \tag{45}$$

$$\delta_y U^{\gamma}_{\alpha,\beta} \coloneqq \frac{U^{\gamma}_{\alpha,\beta+\frac{1}{2}} - U^{\gamma}_{\alpha,\beta-\frac{1}{2}}}{\Delta y}. \tag{46}$$

Next, we define the L^2 normed spaces

$$\mathbb{V}_E \coloneqq \left\{ \mathbf{F} : \tau_h^{E_x} \times \tau_h^{E_y} \longrightarrow \mathbb{R}^2 \mid \mathbf{F} = (F_{x_{l+\frac{1}{2},j}}, F_{y_{l,j+\frac{1}{2}}})^T, \|\mathbf{F}\|_E < \infty \right\} \tag{47}$$

$$\mathbb{V}_H \coloneqq \left\{ U : \tau_h^H \longrightarrow \mathbb{R} \mid U = (U_{l+\frac{1}{2},j+\frac{1}{2}}), \|U\|_H < \infty \right\} \tag{48}$$

with the following discrete norms and inner products

$$\|\mathbf{F}\|_E^2 = \Delta x \Delta y \sum_{\ell=0}^{\ell_{max}-1} \sum_{j=0}^{j_{max}-1} \left(|F_{x_{\ell+\frac{1}{2},j}}|^2 + |F_{y_{\ell,j+\frac{1}{2}}}|^2 \right), \forall\, \mathbf{F} \in \mathbb{V}_E \tag{49}$$

$$(\mathbf{F}, \mathbf{G})_E = \Delta x \Delta y \sum_{\ell=0}^{\ell_{max}-1} \sum_{j=0}^{j_{max}-1} \left(F_{x_{\ell+\frac{1}{2},j}} G_{x_{\ell+\frac{1}{2},j}} + F_{y_{\ell,j+\frac{1}{2}}} G_{y_{\ell,j+\frac{1}{2}}} \right), \forall\, \mathbf{F}, \mathbf{G} \in \mathbb{V}_E \tag{50}$$

$$\|U\|_H^2 = \Delta x \Delta y \sum_{\ell=0}^{\ell_{max}-1} \sum_{j=0}^{j_{max}-1} |U_{\ell+\frac{1}{2},j+\frac{1}{2}}|^2, \forall\, U \in \mathbb{V}_H \tag{51}$$

$$(U, V)_H = \Delta x \Delta y \sum_{\ell=0}^{\ell_{max}-1} \sum_{j=0}^{j_{max}-1} U_{\ell+\frac{1}{2},j+\frac{1}{2}} V_{\ell+\frac{1}{2},j+\frac{1}{2}}, \forall\, U, V \in \mathbb{V}_H. \tag{52}$$

Finally, we define discrete curl operators on the staggered L^2 normed spaces as

$$\begin{aligned} &\mathrm{curl_h} : \mathbb{V}_E \longrightarrow \mathbb{V}_H \qquad && \mathbf{curl_h} : \mathbb{V}_H \longrightarrow \mathbb{V}_E \\ &\mathrm{curl_h}\mathbf{F} \coloneqq \delta_x F_y - \delta_y F_x \qquad && \mathbf{curl_h} U \coloneqq (\delta_y U, -\delta_x U)^T. \end{aligned} \tag{53}$$

We require that PEC conditions hold for all $\mathbf{F} \in \mathbb{V}_E$ so that

$$F_{x_{\ell+\frac{1}{2},0}} = F_{x_{\ell+\frac{1}{2},J}} = 0, \qquad 0 \le \ell \le \ell_{max} \tag{54}$$

$$F_{y_{0,j+\frac{1}{2}}} = F_{x_{L,j+\frac{1}{2}}} = 0, \qquad 0 \le j \le j_{max}. \tag{55}$$

Then discrete integration by parts shows that Green's curl identity holds for our discrete system as well:

$$(\mathrm{curl}_h \mathbf{E}, H)_H = (\mathbf{E}, \mathbf{curl}_h H)_E. \tag{56}$$

The definitions are tedious, but we see that all discrete operators, spaces, and inner products are closely related to the continuous case, as discussed in the previous section.

5.2.2. 2D Yee scheme

Utilizing the operators defined in (43)–(46), we can write out the discrete forms of (27):

$$\delta_t H^n_{\ell+\frac{1}{2},j+\frac{1}{2}} = \frac{1}{\mu_0} \left(\delta_y E^n_{x_{\ell+\frac{1}{2},j+\frac{1}{2}}} - \delta_x E^n_{y_{\ell+\frac{1}{2},j+\frac{1}{2}}} \right) \tag{57a}$$

$$\epsilon_0 \epsilon_\infty \delta_t E^{n+\frac{1}{2}}_{x_{\ell+\frac{1}{2},j}} = \delta_y H^{n+\frac{1}{2}}_{\ell+\frac{1}{2},j} - \vec{\overline{\beta}}^{\,n+\frac{1}{2}}_{0,x_{\ell+\frac{1}{2},j}} \tag{57b}$$

$$\epsilon_0 \epsilon_\infty \delta_t E^{n+\frac{1}{2}}_{y_{\ell,j+\frac{1}{2}}} = -\delta_x H^{n+\frac{1}{2}}_{\ell,j+\frac{1}{2}} - \vec{\overline{\beta}}^{\,n+\frac{1}{2}}_{0,y_{\ell,j+\frac{1}{2}}} \tag{57c}$$

$$\delta_t \vec{\alpha}^{\,n+\frac{1}{2}}_{x_{\ell+\frac{1}{2},j}} = \vec{\overline{\beta}}^{\,n+\frac{1}{2}}_{x_{\ell+\frac{1}{2},j}} \tag{57d}$$

$$\delta_t \vec{\alpha}^{\,n+\frac{1}{2}}_{y_{\ell,j+\frac{1}{2}}} = \vec{\overline{\beta}}^{\,n+\frac{1}{2}}_{y_{\ell,j+\frac{1}{2}}} \tag{57e}$$

$$\delta_t \vec{\beta}_{x_{\ell+\frac{1}{2},j}}^{\,n+\frac{1}{2}} = -\omega_0^2 \overline{\vec{\alpha}}_{x_{\ell+\frac{1}{2},j}}^{\,n+\frac{1}{2}} - 2\nu \overline{\vec{\beta}}_{x_{\ell+\frac{1}{2},j}}^{\,n+\frac{1}{2}} + \hat{e}_1 \epsilon_0 \omega_p^2 \overline{E}_{x_{\ell+\frac{1}{2},j}}^{\,n+\frac{1}{2}} \tag{57f}$$

$$\delta_t \vec{\beta}_{y_{\ell,j+\frac{1}{2}}}^{\,n+\frac{1}{2}} = -\omega_0^2 \overline{\vec{\alpha}}_{y_{\ell,j+\frac{1}{2}}}^{\,n+\frac{1}{2}} - 2\nu \overline{\vec{\beta}}_{y_{\ell,j+\frac{1}{2}}}^{\,n+\frac{1}{2}} + \hat{e}_1 \epsilon_0 \omega_p^2 \overline{E}_{y_{\ell,j+\frac{1}{2}}}^{\,n+\frac{1}{2}}. \tag{57g}$$

However, we can simplify the work by writing the equations in vector notation, where we recall that $\mathbf{F} \in \mathbb{V}_E$ are defined on $\tau_h^{Ex} \times \tau_h^{Ey}$ and $U \in \mathbb{V}_H$ are defined on τ_h^H:

$$\delta_t H^n + \frac{1}{\mu_0}\left(\mathrm{curl}_h \mathbf{E}^n\right) = 0 \tag{58a}$$

$$\epsilon_0 \epsilon_\infty \delta_t \mathbf{E}^{n+\frac{1}{2}} = \left(\mathbf{curl}_h H^{n+\frac{1}{2}}\right) - \hat{e}_1^T \overline{\vec{\beta}}^{\,n+\frac{1}{2}} \tag{58b}$$

$$\delta_t \vec{\boldsymbol{\alpha}}^{n+\frac{1}{2}} = \overline{\vec{\beta}}^{\,n+\frac{1}{2}} \tag{58c}$$

$$\delta_t \vec{\boldsymbol{\beta}}^{n+\frac{1}{2}} = -\omega_0^2 \overline{\vec{\alpha}}^{\,n+\frac{1}{2}} - 2\nu \overline{\vec{\beta}}^{\,n+\frac{1}{2}} + \hat{e}_1 \epsilon_0 \omega_p^2 \overline{\mathbf{E}}^{n+\frac{1}{2}}. \tag{58d}$$

We must also define another space and inner product for the random polarization in vector notation as $\vec{\alpha}$ and $\vec{\beta}$ are now $2 \times p$ matrices:

$$\mathbb{V}_\alpha := \left\{ \vec{\boldsymbol{\alpha}} : \tau_h^{Ex} \times \tau_h^{Ey} \longrightarrow \mathbb{R}^2 \times \mathbb{R}^p \;\middle|\; \vec{\boldsymbol{\alpha}} = [\boldsymbol{\alpha}_0, \ldots, \boldsymbol{\alpha}_{p-1}], \boldsymbol{\alpha}_k \in \mathbb{V}_E, \|\vec{\boldsymbol{\alpha}}\|_\alpha < \infty \right\}$$

where the discrete L^2 grid norm and inner product are defined as

$$\|\vec{\boldsymbol{\alpha}}\|_\alpha^2 = \sum_{k=0}^{p-1} \|\boldsymbol{\alpha}_k\|_E^2, \quad \forall\, \vec{\boldsymbol{\alpha}} \in \mathbb{V}_\alpha$$

$$(\vec{\boldsymbol{\alpha}}, \vec{\boldsymbol{\beta}})_\alpha = \sum_{k=0}^{p-1} \left(\boldsymbol{\alpha}_k, \boldsymbol{\beta}_k\right)_E, \quad \forall\, \vec{\boldsymbol{\alpha}}, \vec{\boldsymbol{\beta}} \in \mathbb{V}_\alpha.$$

5.2.3. Energy decay and stability

We choose both spacial steps to be equal ($\Delta x = \Delta y = h$), and require that the usual CFL condition for two dimensions holds:

$$\sqrt{2} c_\infty \Delta t \le h. \tag{59}$$

Theorem 5.2 (*Energy Decay for Maxwell-PC Lorentz-FDTD*)**.** *If the stability condition (59) is satisfied, then the Yee scheme for the 2D TE mode Maxwell-PC Lorentz system given in (57) satisfies the discrete identity*

$$\delta_t \mathcal{E}_h^{n+\frac{1}{2}} = \frac{-1}{\overline{\mathcal{E}}_h^{n+\frac{1}{2}}} \left\| \sqrt{\frac{2\nu}{\epsilon_0 \omega_p^2}} \overline{\vec{\beta}}_h^{\,n+\frac{1}{2}} \right\|_\alpha^2 \tag{60}$$

for all n where

$$\mathcal{E}_h^n = \left(\mu_0 (H^{n+\frac{1}{2}}, H^{n-\frac{1}{2}})_H + \left\| \sqrt{\epsilon_0 \epsilon_\infty}\, \mathbf{E}^n \right\|_E^2 + \left\| \sqrt{\frac{\omega_0^2}{\epsilon_0 \omega_p^2}} \vec{\alpha}^n \right\|_\alpha^2 + \left\| \sqrt{\frac{1}{\epsilon_0 \omega_p^2}} \vec{\beta}^n \right\|_\alpha^2 \right)^{1/2} \tag{61}$$

defines a discrete energy.

Proof. Multiplying both sides of (58b) by $\Delta x \Delta y \overline{\mathbf{E}}^{n+\frac{1}{2}}$ and summing over all nodes on $\tau_h^{Ex} \times \tau_h^{Ey}$, we obtain

$$\epsilon_0 \epsilon_\infty (\delta_t \mathbf{E}^{n+\frac{1}{2}}, \overline{\mathbf{E}}^{n+\frac{1}{2}})_E = (\mathbf{curl}_h H^{n+\frac{1}{2}}, \overline{\mathbf{E}}^{n+\frac{1}{2}})_E - (\hat{e}_1^T \overline{\vec{\beta}}^{\,n+\frac{1}{2}}, \overline{\mathbf{E}}^{n+\frac{1}{2}})_E \tag{62}$$

which is equivalent to

$$\frac{\epsilon_0 \epsilon_\infty}{2\Delta t}\left[\|\mathbf{E}^{n+1}\|_E^2 - \|\mathbf{E}^n\|_E^2 \right] = (\mathbf{curl}_h H^{n+\frac{1}{2}}, \overline{\mathbf{E}}^{n+\frac{1}{2}})_E - (\hat{e}_1^T \overline{\vec{\beta}}^{\,n+\frac{1}{2}}, \overline{\mathbf{E}}^{n+\frac{1}{2}})_E. \tag{63}$$

Next, we take the average of (58a) at n and $n+1$, multiply by $\Delta x \Delta y H^{n+\frac{1}{2}}$, and sum over τ_h^H to get

$$\mu_0 (\delta_t \overline{H}^{n+\frac{1}{2}}, H^{n+\frac{1}{2}})_H + (\mathrm{curl}_h \overline{\mathbf{E}}^{n+\frac{1}{2}}, H^{n+\frac{1}{2}})_H = 0 \tag{64}$$

which is equivalent to

$$\frac{\mu_0}{2\Delta t}\left[(H^{n+\frac{3}{2}}, H^{n+\frac{1}{2}})_H - (H^{n+\frac{1}{2}}, H^{n-\frac{1}{2}})_H\right] + (\mathrm{curl}_h \overline{\mathbf{E}}^{n+\frac{1}{2}}, H^{n+\frac{1}{2}})_H = 0. \tag{65}$$

Multiplying (58c) by $\Delta x \Delta y \vec{\overline{\alpha}}^{n+\frac{1}{2}}$ and summing over $\tau_h^{E_x} \times \tau_h^{E_y}$, we get

$$\left(\delta_t \vec{\boldsymbol{\alpha}}^{n+\frac{1}{2}}, \vec{\overline{\boldsymbol{\alpha}}}^{\,n+\frac{1}{2}}\right)_\alpha = \left(\vec{\overline{\beta}}^{n+\frac{1}{2}}, \vec{\overline{\boldsymbol{\alpha}}}^{\,n+\frac{1}{2}}\right)_\alpha. \tag{66}$$

We multiply by $\frac{\omega_0^2}{\epsilon_0 \omega_p^2}$ and rewrite as

$$\frac{\omega_0^2}{2\Delta t \epsilon_0 \omega_p^2}\left[\|\vec{\boldsymbol{\alpha}}^{n+1}\|_\alpha^2 - \|\vec{\boldsymbol{\alpha}}^{n}\|_\alpha^2\right] = \frac{\omega_0^2}{\epsilon_0 \omega_p^2}\left(\vec{\overline{\beta}}^{n+\frac{1}{2}}, \vec{\overline{\boldsymbol{\alpha}}}^{\,n+\frac{1}{2}}\right)_\alpha. \tag{67}$$

Lastly, we multiply (58d) by $\Delta x \Delta y \vec{\overline{\beta}}^{n+\frac{1}{2}}$ and sum over $\tau_h^{E_x} \times \tau_h^{E_y}$ to obtain

$$\begin{aligned}&\left(\delta_t \vec{\boldsymbol{\beta}}^{n+\frac{1}{2}}, \vec{\overline{\boldsymbol{\beta}}}^{\,n+\frac{1}{2}}\right)_\alpha = \\ &-\omega_0^2\left(\vec{\overline{\alpha}}^{n+\frac{1}{2}}, \vec{\overline{\boldsymbol{\beta}}}^{\,n+\frac{1}{2}}\right)_\alpha - 2\nu\left(\vec{\overline{\beta}}^{n+\frac{1}{2}}, \vec{\overline{\boldsymbol{\beta}}}^{\,n+\frac{1}{2}}\right)_\alpha + \left(\hat{e}_1 \epsilon_0 \omega_p^2 \overline{\mathbf{E}}^{n+\frac{1}{2}}, \vec{\overline{\boldsymbol{\beta}}}^{\,n+\frac{1}{2}}\right)_\alpha.\end{aligned} \tag{68}$$

We multiply by $\frac{1}{\epsilon_0 \omega_p^2}$ and rewrite as

$$\begin{aligned}&\frac{1}{2\Delta t \epsilon_0 \omega_p^2}\left[\|\vec{\boldsymbol{\beta}}^{n+1}\|_\alpha^2 - \|\vec{\boldsymbol{\beta}}^{n}\|_\alpha^2\right] = \\ &\frac{-\omega_0^2}{\epsilon_0 \omega_p^2}\left(\vec{\overline{\alpha}}^{n+\frac{1}{2}}, \vec{\overline{\boldsymbol{\beta}}}^{\,n+\frac{1}{2}}\right)_\alpha - \frac{2\nu}{\epsilon_0 \omega_p^2}\left(\vec{\overline{\beta}}^{n+\frac{1}{2}}, \vec{\overline{\boldsymbol{\beta}}}^{\,n+\frac{1}{2}}\right)_\alpha + \left(\hat{e}_1 \overline{\mathbf{E}}^{n+\frac{1}{2}}, \vec{\overline{\boldsymbol{\beta}}}^{\,n+\frac{1}{2}}\right)_\alpha.\end{aligned} \tag{69}$$

Adding (63), (65), (67), and (69), then using the definition (61), we have

$$\frac{1}{2\Delta t}\left\{(\mathcal{E}_h^{n+1})^2 - (\mathcal{E}_h^{n})^2\right\} = -\frac{2\nu}{\epsilon_0 \omega_p^2}\left(\vec{\overline{\beta}}^{n+\frac{1}{2}}, \vec{\overline{\boldsymbol{\beta}}}^{\,n+\frac{1}{2}}\right)_\alpha \tag{70}$$

where we noticed that

$$(\hat{e}_1 \overline{\mathbf{E}}^{n+\frac{1}{2}}, \vec{\overline{\boldsymbol{\beta}}}^{\,n+\frac{1}{2}})_\alpha = (\hat{e}_1^T \vec{\overline{\beta}}^{n+\frac{1}{2}}, \overline{\mathbf{E}}^{n+\frac{1}{2}})_E.$$

We can rewrite (70) in the form

$$\frac{\mathcal{E}_h^{n+1} - \mathcal{E}_h^{n}}{\Delta t} = -\left(\frac{2}{\mathcal{E}_h^{n+1} + \mathcal{E}_h^{n}}\right)\left\|\sqrt{\frac{2\nu}{\epsilon_0 \omega_p^2}}\vec{\overline{\beta}}^{n+\frac{1}{2}}\right\|_\alpha^2, \tag{71}$$

where it is assumed that $\mathcal{E}_h^n > 0$ for any n. We prove that (61) is a discrete energy (or positive definite function) by rewriting as

$$(\mathcal{E}_h^n)^2 = \mu_0 \|\overline{H}^n\|_H^2 + \epsilon_0 \epsilon_\infty (\mathbf{E}^n, \mathcal{A}_h \mathbf{E}^n)_E + \frac{1}{\epsilon_0 \omega_p^2}\left(\omega_0 \vec{\overline{\alpha}}^{n}, \omega_0 \vec{\overline{\alpha}}^{n}\right)_\alpha + \frac{2\nu}{\epsilon_0 \omega_p^2}\left(\vec{\overline{\beta}}_h^{n+\frac{1}{2}}, \vec{\overline{\beta}}_h^{n+\frac{1}{2}}\right)_\alpha \tag{72}$$

where $\mathcal{A}_h$ is positive definite when the CFL condition is satisfied. The details follow similarly to [20]. □

6. Dispersion analysis

6.1. Exact dispersion for random Lorentz

We plug the plane wave solutions $V(t, x, y) = \tilde{V} e^{i(x k_x + y k_y - \omega t)}$ into the Random Lorentz system. After rearranging terms we get:

$$\omega \mu_0 \tilde{H} = k_x \tilde{E}_y - k_y \tilde{E}_x \tag{73a}$$

$$\epsilon_0 \epsilon_\infty \tilde{E}_x = -\frac{k_y}{w}\tilde{H} - \tilde{P}_x \tag{73b}$$

$$\epsilon_0\epsilon_\infty\tilde{E}_y = -\frac{k_x}{w}\tilde{H} - \tilde{P}_y \tag{73c}$$

$$\tilde{\mathcal{P}}_x = \frac{\epsilon_0\omega_p^2\tilde{E}_x}{\omega_0^2 - \omega^2 + i2\nu\omega} \tag{73d}$$

$$\tilde{\mathcal{P}}_y = \frac{\epsilon_0\omega_p^2\tilde{E}_y}{\omega_0^2 - \omega^2 + i2\nu\omega}. \tag{73e}$$

We take $\tilde{P} = \mathbf{E}(\tilde{\mathcal{P}})$ where ω_0^2 is the random variable. Plugging (73d) into (73b) and (73e) into (73c) we find:

$$\omega\mu_0\tilde{H} = k_x\tilde{E}_y - k_y\tilde{E}_x \tag{74a}$$

$$\epsilon_0\epsilon\tilde{E}_x = -\frac{k_y}{\omega}\tilde{H} \tag{74b}$$

$$\epsilon_0\epsilon\tilde{E}_y = \frac{k_x}{\omega}\tilde{H} \tag{74c}$$

$$\epsilon = \epsilon_\infty + \omega_p^2\mathbb{E}\left(\frac{1}{\omega_0^2 - \omega^2 + i2\nu\omega}\right) \tag{74d}$$

where, in particular, (74d) gives the *expected complex permittivity*. Finally, plugging (74b) and (74c) into (74a), we find the dispersion relation for the Random Lorentz system

$$\frac{\omega^2}{c^2}\epsilon = k^2 \tag{75}$$

where $\epsilon_0\mu_0 = \frac{1}{c^2}$ and $k^2 = k_x^2 + k_y^2$.

6.2. Lorentz PC dispersion

We assume plane wave solutions of all the field variables such that $V_{\ell,j}^n = \tilde{V}e^{i\left(\ell\Delta x k_{x,\Delta} + j\Delta y k_{y,\Delta} - \omega n\Delta t\right)}$. For simplicity, we define the following terms:

$$\omega_\Delta = \frac{2}{\Delta t}\sin\left(\frac{\omega\Delta t}{2}\right),\ K_{x,\Delta} = \frac{2}{\Delta x}\sin\left(\frac{k_{x,\Delta}\Delta x}{2}\right),\ K_{y,\Delta} = \frac{2}{\Delta y}\sin\left(\frac{k_{y,\Delta}\Delta y}{2}\right). \tag{76}$$

Plugging the plane wave solutions into the PC-Random Lorentz model and simplifying gets:

$$-\mu_0\tilde{H}\omega_\Delta = \tilde{E}_x K_{y,\Delta} - \tilde{E}_y K_{x,\Delta} \tag{77a}$$

$$\tilde{\epsilon}\tilde{E}_x\omega_\Delta = -\tilde{H}K_{y,\Delta} - i\tilde{\beta}_{0,x}\cos\left(\frac{\omega\Delta t}{2}\right) \tag{77b}$$

$$\tilde{\epsilon}\tilde{E}_y\omega_\Delta = \tilde{H}K_{x,\Delta} - i\tilde{\beta}_{0,y}\cos\left(\frac{\omega\Delta t}{2}\right) \tag{77c}$$

$$\tilde{\alpha}_x\omega_\Delta = i\tilde{\beta}_x\cos\left(\frac{\omega\Delta t}{2}\right) \tag{77d}$$

$$\tilde{\alpha}_y\omega_\Delta = i\tilde{\beta}_y\cos\left(\frac{\omega\Delta t}{2}\right) \tag{77e}$$

$$\tilde{\beta}_x\omega_\Delta = (-iA\alpha_x - i2\nu\tilde{\beta}_x + \hat{e}_1 i\epsilon_0\omega_p^2\tilde{E}_x)\cos\left(\frac{\omega\Delta t}{2}\right) \tag{77f}$$

$$\tilde{\beta}_y\omega_\Delta = (-iA\alpha_y - i2\nu\tilde{\beta}_y + \hat{e}_1 i\epsilon_0\omega_p^2\tilde{E}_y)\cos\left(\frac{\omega\Delta t}{2}\right). \tag{77g}$$

We now add additional notation for the discrete misrepresentation of the model parameters

$$A_\Delta = A\cos^2\left(\frac{\omega\Delta t}{2}\right),\ \nu_\Delta = \nu\cos\left(\frac{\omega\Delta t}{2}\right),\ \text{and } \omega_{p,\Delta} = \omega_p\cos\left(\frac{\omega\Delta t}{2}\right). \tag{78}$$

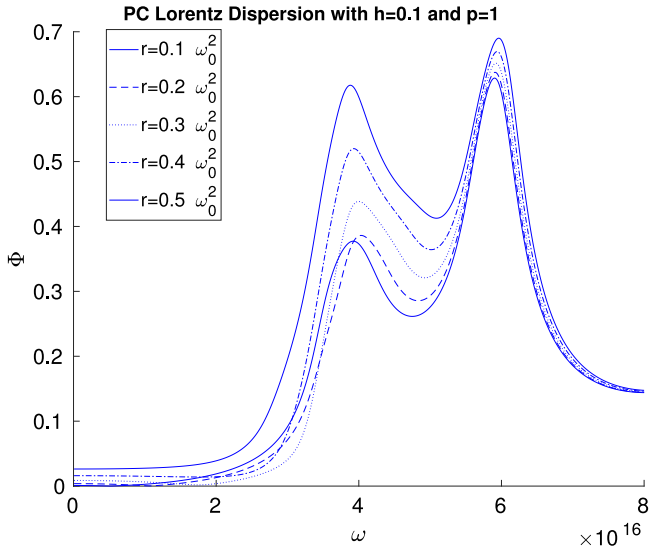

Fig. 3. Plots of phase error with varying r using $h = 0.1$ and $P = 1$.

Next we insert (77d) into (77f) and (77e) into (77g) and solve for $\tilde{\beta}_{x,0}$ and $\tilde{\beta}_{y,0}$ to get:

$$\tilde{\beta}_{x,0} = -i\hat{e}_1^T \left(A_\Delta - \omega_\Delta^2 I - i2\nu_\Delta\omega_\Delta I\right)^{-1} \hat{e}_1\epsilon_0\omega_\Delta\omega_p^2\tilde{E}_x \cos\left(\frac{\omega\Delta t}{2}\right) \tag{79a}$$

$$\tilde{\beta}_{y,0} = -i\hat{e}_1^T \left(A_\Delta - \omega_\Delta^2 I - i2\nu_\Delta\omega_\Delta I\right)^{-1} \hat{e}_1\epsilon_0\omega_\Delta\omega_p^2\tilde{E}_y \cos\left(\frac{\omega\Delta t}{2}\right), \tag{79b}$$

where I is the identity matrix.

Plugging (79a) into (77b) and (79b) into (77c), we find:

$$\tilde{E}_x\epsilon_0\omega_\Delta\epsilon\Delta = -\tilde{H}K_{y,\Delta} \tag{80a}$$

$$\tilde{E}_y\epsilon_0\omega_\Delta\epsilon\Delta = \tilde{H}K_{x,\Delta} \tag{80b}$$

$$\epsilon_\Delta = \epsilon_\infty + \omega_{p,\Delta}^2\, \hat{e}_1^T \left(A_\Delta - \omega_\Delta^2 I - i2\nu_\Delta\omega_\Delta I\right)^{-1} \hat{e}_1 \tag{80c}$$

where, in particular, (80c) gives the *discrete expected complex permittivity*. Note that the relation has a similar form to (74d) in that the matrix inverse takes the place of division and the pre and post multiplication by $\hat{e}_1$, the first standard unit normal vector, has the effect of taking an expected value. Finally, we insert (80a) and (80b) into (77a) to find the discrete dispersion relation

$$\frac{\omega_\Delta^2}{c^2}\epsilon_\Delta = k_\Delta^2, \tag{81}$$

where $k_\Delta^2 = K_{x,\Delta}^2 + K_{y,\Delta}^2$.

6.3. Dispersion error

The exact dispersion relation can be compared with a discrete dispersion relation to determine the amount of dispersion error. We define the phase error Φ for a scheme applied to a model to be

$$\Phi = \left|\frac{k - k_\Delta}{k}\right|, \tag{82}$$

where the numerical wave number k_Δ is implicitly determined by the discrete dispersion relation (81) with (80c) and k is the exact wave number for the model implicitly defined by (75) with (74d). We wish to examine the phase error as a function of ω in the range around $\overline{\omega}_0$ (depicted with an overbar to indicate that it is a parameter of the distribution of ω_0^2, in particular, the square root of the midpoint of the distribution). The discretization parameter Δt is determined by the dimensionless scaling parameter $h := \overline{\omega}_0\Delta t/(2\pi)$, while $\Delta x = \Delta y$ are determined by the CFL condition after Δt has been determined. The parameter r indicates the variability of the random variable $\omega_0^2 := \overline{\omega}_0^2 + r\xi,\ \xi \in (-1, 1)$. (In

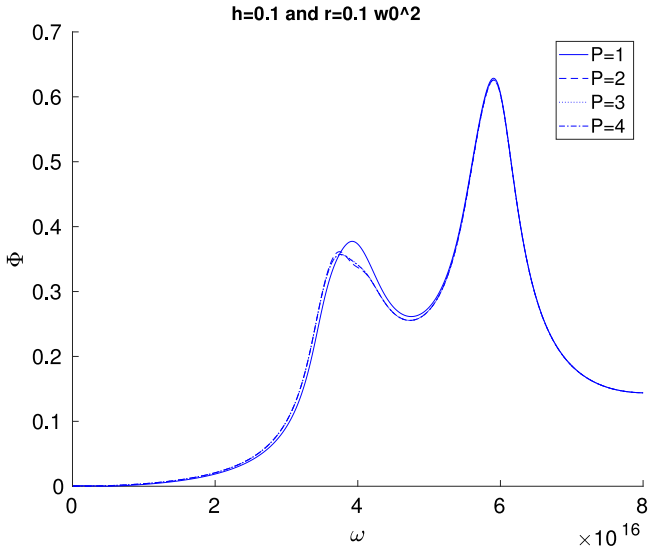

Fig. 4. Plots of phase error varying P using $h = 0.1$ and $r = 0.1$.

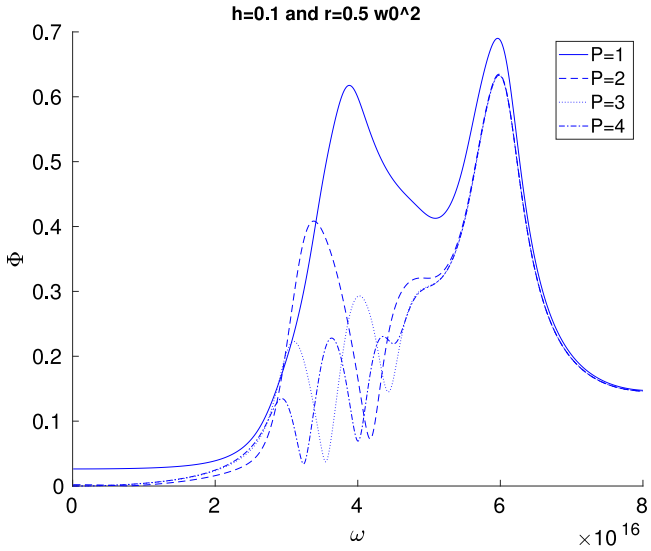

Fig. 5. Plots of phase error varying P using $h = 0.1$ and $r = 0.5$.

the numerical examples below, we use a relative value of r, for instance $r = 0.1\ \overline{\omega}_0^2$. The work in [18,19] showed that $r = 0.0855$ is reasonable for modeling saltwater data in the frequency domain.)

We assume a uniform distribution for simplicity and the following realistic material parameters [13]

$$\epsilon_\infty = 1, \quad \epsilon_s = 2.25, \quad \nu = 2.8 \times 10^{15}\ 1/\text{s}, \quad \overline{\omega}_0 = 4 \times 10^{16}\ \text{rad/s}.$$

Fig. 3 shows the effect of the width of the random distribution of ω_0^2 by fixing the number of terms in the polynomial chaos expansion ($P = 1$ means linear polynomials) and the scaling parameter $h = 0.1$. As expected, the lower variability in the dielectric parameter yields the lesser dispersion error since only two terms of PCE cannot be expected to well represent a random effect with such variability. Figs. 4 and 5 show the convergence in degree of PCE. In particular, for low variability, $r = 0.1$ three terms is sufficient to reduce the dispersion error down to the baseline for this choice of discretization parameters. In other words, there is a contribution to the dispersion error from the spatial, temporal and spectral discretizations, and here the spectral contribution is less than the others for $P > 2$. For high variability, $r = 0.5$, there is a persistent contribution to the dispersion error from the spectral discretization for at least P up to 4. Figs. 6 and 7 repeat the two previous cases but reduce the time step by a factor of 10 (thus, also the spatial step). Thus the contributions to the dispersion error from space and time discretizations are reduced, and higher resolution in random

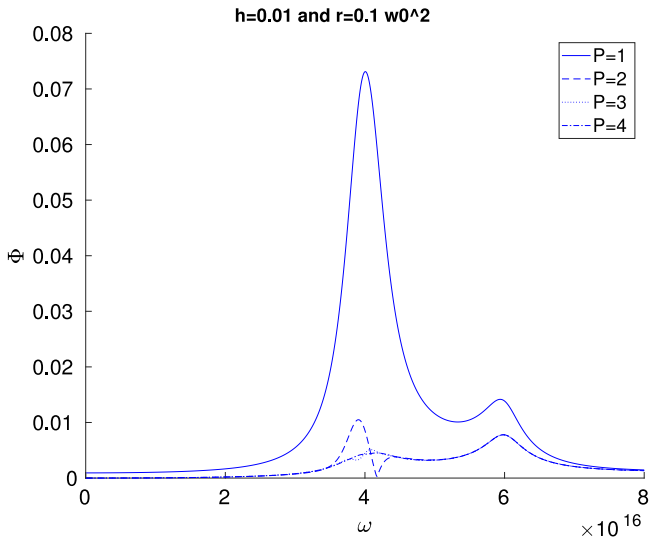

Fig. 6. Plots of phase error varying P using $h = 0.01$ and $r = 0.1$.

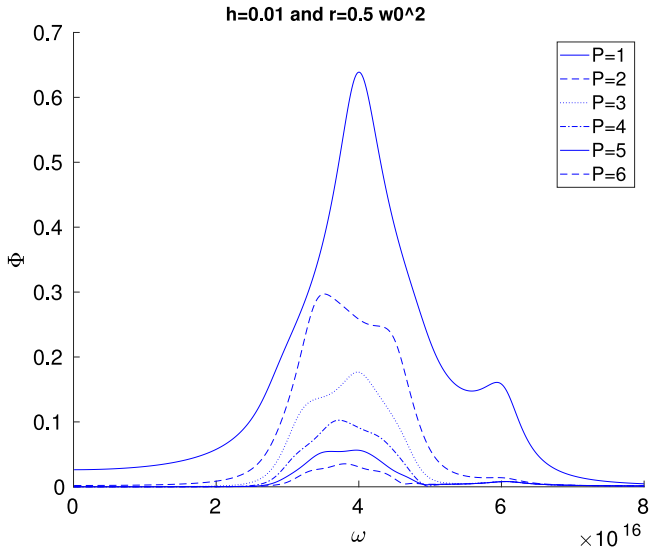

Fig. 7. Plots of phase error varying P using $h = 0.01$ and $r = 0.5$.

space is necessary to similarly reduce the spectral contribution to dispersion error. For the low variability case, $P = 3$ is sufficient; for the high variability case, there is still a non-negligible contribution even with $P = 6$. Finally, Fig. 8 shows an addition decrease in the space and time discretization steps, and again $P = 3$ appears to be sufficient for reducing the spectral contribution to dispersion error down to the baseline in the low variability case.

7. Conclusion and future work

We have used Polynomial Chaos Expansions to discretize in random space the auxiliary differential equation for the Lorentz polarization model which includes distributions of dielectric parameters. Using the Yee Scheme to fully discretize the Random Lorentz system in the time domain, we provided simulations which show fast convergence in the degree of polynomials used in the expansion. We have shown the stability of the random system, and that the numerical approach maintains the conditional stability of the Yee scheme for Lorentz materials. We have also derived the discrete dispersion relation which allows the phase error to be computed. Results were provided in one and two dimensions, but the approach is easily extendable to three dimensions.

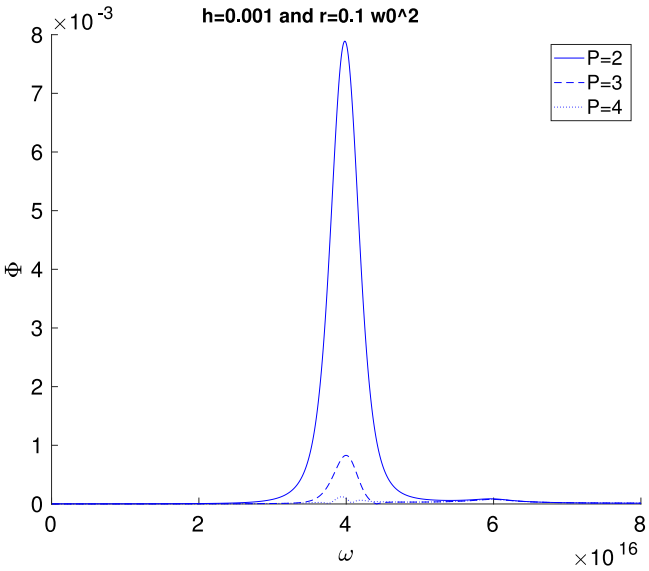

Fig. 8. Plots of phase error varying P using $h = 0.001$ and $r = 0.1$.

Declaration of competing interest

The authors declare that they have no known competing financial interests or personal relationships that could have appeared to influence the work reported in this paper.

CRediT authorship contribution statement

Andrew Fisher: Software, Formal analysis, Writing - original draft, Visualization. **Jacqueline Alvarez:** Investigation, Writing - review & editing. **N.L. Gibson:** Methodology, Supervision, Writing - review & editing.

Acknowledgments

This work was performed during the 2017 REU program in mathematics at Oregon State University, with support by National Science Foundation Grant DMS-1359173.

References

[1] Banks HT, Catenacci J, Hu S. Method comparison for estimation of distributed parameters in permittivity models using reflectance. Eurasian J Math Comput Appl 2015;3(2):4–24.
[2] Gibson NL. A polynomial chaos method for dispersive electromagnetics. Commun Comput Phys 2015;18(5):1234–63.
[3] Foster KR, Schwan HP. Dielectric properties of tissues. Handb Biol Effects Electromagn Fields 1996;2:25–102.
[4] Xiu D, Karniadakis G. The Wiener–Askey polynomial chaos for stochastic differential equations. SIAM J Sci Comput 2003;24(2):619–44.
[5] Xiu D. Fast numerical methods for stochastic computations: a review. Commun Comput Phys 2009;5(2–4):242–72.
[6] Xiu D. Numerical methods for stochastic computations. Princeton University Press; 2010.
[7] Yee K. Numerical solution of inital boundary value problems involving Maxwell's equations in isotropic media. IEEE Trans Antennas Propag 1966;14(3):302–7.
[8] Monk P. A convergence analysis of Yee's scheme on nonuniform grids. SIAM J Numer Anal 1994;31(2):393–412.
[9] Joseph RM, Hagness SC, Taflove A. Direct time integration of Maxwell's equations in linear dispersive media with absorption for scattering and propagation of femtosecond electromagnetic pulses. Opt Lett 1991;16(18):1412–4.
[10] Kashiwa T, Yoshida N, Fukai I. A treatment by the finite-difference time domain method of the dispersive characteristics associated with orientational polarization. IEEE Trans IEICE 1990;73(8):1326–8.
[11] Kashiwa T, Fukai I. A treatment by the FD-TD method of the dispersive characteristics associated with electronic polarization. Microw Opt Technol Lett 1990;3(6):203–5.
[12] Young JL, Nelson RO. A summary and systematic analysis of FDTD algorithms for linearly dispersive media. IEEE Antennas Propag Mag 2001;43:61–77.
[13] Banks HT, Buksas MW, Lin T. Electromagnetic material interrogation using conductive interfaces and acoustic wavefronts. SIAM; 2000.
[14] Banks HT, Gibson NL. Electromagnetic inverse problems involving distributions of dielectric mechanisms and parameters. Quart Appl Math 2006;64(4):749–95.
[15] Chauvière C, Hesthaven JS, Lurati L. Computational modeling of uncertainty in time-domain electromagnetics. SIAM J Sci Comput 2006;28(2):751–75.
[16] Li J, Fang Z, Lin G. Regularity analysis of metamaterial Maxwell's equations with random coefficients and initial conditions. Comput Methods Appl Mech Engrg 2018;335:24–51.
[17] Fang Z, Li J, Tang T, Zhou T. Efficient stochastic Galerkin methods for Maxwell's equations with random inputs. J Sci Comput 2019;80(1):248–67.

[18] Alvarez J, Fisher A. Approximating dispersive materials with parameter distributions in the Lorentz model. In: Gibson NL, editor. REU program at Oregon State University proceedings. 2017.
[19] Alvarez J, Fisher A, Gibson NL. Approximating Dispersive Materials With Parameter Distributions in the Lorentz Model. Submitted for publication.
[20] Bokil VA, Gibson NL. Convergence analysis of Yee schemes for Maxwell's equations in Debye and Lorentz dispersive media. Int J Numer Anal Model 2014;11(4):657–87.